

Some of this paper's results are also applicable to magnetotugger-based attitude control of momentum-biased spinning spacecraft. Such systems have (almost) periodic models that are similar to those of the present study, and it is possible to design controllers for such systems using the new methods that are presented here.

Other studies have considered acaricidal saturation^{9,12} or integral¹⁻⁴ control actions.⁵ This is the first paper to consider them together. Simultaneous consideration of these issues is important because integrators can cause stability problems when control sat-

This paper's approximate LQR solution is similar to the constant gain solution that is presented in Ref. 11. The present development makes a stronger connection to an underlying periodic LQR problem. This connection allows the design to be modified so that it can parametrize model uncertainties.

micromechanics microgradients in its surroundings, which creates effects of disturbances. Third, it develops a way to ensure stability in the presence of actuator saturation—this is a first for any time-varying control law, not just for the magnetic attitude control problem. Last, it evaluates the controllers robustness with respect

The present study makes four important contributions to three-axis magnetic attitude control. First, it develops a time-varying, full-state-feedback LQR control law that is based on a constant approximation solution of the time-varying Riccati equation. Second, it provides a controller which contains the steady-state solution of the Riccati equation.

Various control laws have been considered for magnetic attitude control systems. Some of the controllers are similar to the original controller of Ref. 7,^{10,14} Time-varying linear quadratic regulator (LQR) formulations have been used.^{5,8,11} A time-invariant LQR problem, Ref. 9 and 13, has fuzzy control and solutions that change with time.

The present problem is different from the problem of attitude control when turbines or reaction wheels provide torque only about two axes. References 1-7 and others have addressed this ultimate problem, in which the unactuated direction is defined in space rather than in the vehicle's body frame. For magnetic torques the unactuated direction is de-

that is approximately periodic. This system's underlying structure and periodicity combine to create a challenging feedback controller problem.

A method of using magnetic torque rods to do three-axis spacecraft attitude control has been developed. The goal of this system is to achieve a nadir-pointing accuracy on the order of 0.1–1.0 deg without the need for thrusters or wheels. The open-loop system is underactuated because magnetic torque rods cannot torque about the local magnetic field direction. This direction moves in space as the spacecraft moves along an inclined orbit, and the resulting system is roughly periodic. Periodic controllers are designed using an asymptotic linear quadratic regulator technique. The control laws include integral action and saturation logic. This concept has been studied via analysis and simulation. The resulting closed-loop systems exhibit robustness with respect to parameter modeling uncertainty. They converge from initial attitude errors of 30 deg per axis, and they achieve steady-state pointing errors on the order of 0.5–1.0 deg in the presence of drag torques and unmodeled residual dipole moments.

Cornell University, Ithaca, New York 14853-7501

Magnetic Torquer Attitude Control via Asymptotic Periodic Linear Quadratic Regulation

In these equations ϕ , θ and ψ are the roll, pitch, and yaw angles, L_x , L_y , L_z respectively, and m_0 is the orbital rate. I_{xx} is the moment of inertia about the principal axis, I_{yy} is the moment of inertia about the pitch axis, and I_{zz} is the moment of inertia about the yaw axis. The magnetic field vector \mathbf{B} is given by $B_x = B \cos \theta \sin \psi$, $B_y = B \sin \theta \sin \psi$, and $B_z = B \cos \psi$. The Earth's magnetic field vector \mathbf{B}_E is given by $B_E^x = B_E \cos \theta \sin \psi$, $B_E^y = B_E \sin \theta \sin \psi$, and $B_E^z = B_E \cos \psi$.

$$\begin{aligned}
 (9) \quad & \left[\begin{array}{ccc} 0 & 0 & 0 \\ 0 & 0 & 0 \\ 0 & 0 & 0 \\ 0 & 0 & 0 \\ 0 & 0 & 0 \\ 0 & 0 & 0 \end{array} \right] + \\
 & \left[\begin{array}{ccc} 0 & 0 & 0 \\ 0 & 0 & 0 \\ 0 & 0 & 0 \\ 0 & 0 & 0 \\ 0 & 0 & 0 \\ 0 & 0 & 0 \end{array} \right] + \\
 & \left[\begin{array}{ccc} 0 & -q_1/I_1 & q_2/I_1 \\ q_1/I_1 & 0 & -q_3/I_1 \\ -q_2/I_1 & q_3/I_1 & 0 \\ 0 & 0 & 0 \\ 0 & 0 & 0 \\ 0 & 0 & 0 \end{array} \right] + \left[\begin{array}{c} \sigma_{sc/113} \\ \sigma_{sc/112} \\ \sigma_{sc/111} \\ \phi \\ \theta \\ \phi \end{array} \right] \times \\
 & \left[\begin{array}{cccccc} 0 & 0 & (\xi\sigma + \eta)^{0\omega} & \xi\sigma^{0\omega} & 0 & 0 \\ 0 & 0 & 0 & 0 & \xi\sigma^{0\omega} & 0 \\ 0 & 0 & 0 & 0 & 0 & 0 \\ 0 & 0 & 0 & 0 & 0 & 0 \\ 1 & 0 & 0 & 0 & 0 & 0 \\ 0 & 1 & 0 & 0 & 0 & 0 \\ 0 & 0 & 1 & 0 & 0 & 0 \end{array} \right] - 4\sigma^{0\omega} \left[\begin{array}{c} \sigma_{sc/113} \\ \sigma_{sc/112} \\ \sigma_{sc/111} \\ \phi \\ \theta \\ \phi \end{array} \right]
 \end{aligned}$$

The high-fidelity nonlinear model in Figs. (2a) and (2b) is too complicated for use in control design or in closed-loop stability analysis. Fortunately, a simpler linearized model gives a reasonable approximation of the nonlinear system over a wide range of conditions, i.e., for attitude perturbations up to 30 deg and attitude rate perturbations up to half of the orbital rotation rate. The linearized model assumes a circular orbit, and linearization is performed about the equilibrium nadir-pointing attitude. The linearized model is

Л.Н.Толстой в «Воксе» юношеского

The generic Kepler orbital model has been used with this nonlinear aerodynamic reference area, and C_D is its drag coefficient.

From the 1976 U.S. Standard Atmosphere, ρ_{S} is the function of altitude where $\rho_{\text{SCEF}}(t)$ gives the air density as a function of altitude from the Earth's surface to the center of the planet. The drag is given by

$$f_{\text{drag}} = A_{\infty} / (q) A_l / \text{CEF}(t) - 0.5 \rho_{\text{SCEF}(t)} \|\text{VECF}(t)\| \text{VECF}(t) \cdot \text{SC}_D$$

These vectors are expressed in spacecraft coordinates. The drag is measured with respect to the center of mass, f_{drag} , is the drag force, and m_{resid} is the residual magnetic dipole moment of the spacecraft, in this equation r_{sc} is the position vector of the aerodynamic center and m_{resid} is the center of mass of the system. The drag force is

$$n_d = r_{\text{sc}} \times f_{\text{drag}} + m_{\text{resid}} \times b$$

(4)

The disturbance model includes the aerodynamic drag torque and the effects of residual spacecraft magnetic dipole moment:

Note that b_{ECEF} , the Earth's field in ECEF coordinates, depends on position and time.

The gravity gradient model computes n_{gg} as a function of the spacecraft's position, attitude, and inertia matrix: $n_{\text{gg}} = n_{\text{gg}}^{\text{eff}}$. The ECEF(t), $A_{\text{gg}}/\|A_{\text{gg}}\|$ or ECEF(t), I_3 . This model includes the b_{gg} terms.

$$q = A_{\text{sc}/\text{ll}}(q) A_{\text{ll}/\text{ECF}}(t) q_{\text{ECF}}[P_{\text{ECF}}(t), t] \quad (3)$$

The magnetic field in spacecraft coordinates b is computed using the spacecraft position, the spacecraft attitude, and a spherical harmonic model of the Earth's magnetic field¹⁸:

where Eq. (2a) is the quaternion kinematic equation and Eq. (2b) is Buler's equation of motion for a rigid body. In this model $w = [w_1; w_2; w_3]$ is the rotation rate of the spacecraft-fixed reference frame with respect to inertial coordinates. It is expressed in the spacecraft reference frame. The vector $[w_{\text{S}}/11; w_{\text{S}}/12; w_{\text{S}}/13] = [w - A_{\text{S}}/\|w\| (w \|w\|)]$ is the rotation rate of the spacecraft reference frame with respect to the inertia matrix of the spacecraft. The matrix A_{S} is the inertia matrix of the spacecraft. The 3 \times 3 matrix I is the identity matrix. The 3 \times 1 matrix n_{S} is the gravity-gradient torque, and m_d is the net disturbance moment of inertia.

$$(2b) \quad I\omega + m + q \times u^p + u^q$$

$$\vec{b} = \frac{1}{2} \begin{bmatrix} -\omega_{sc}/11 & -\omega_{sc}/12 & -\omega_{sc}/13 \\ \omega_{sc}/12 & -\omega_{sc}/11 & 0 \\ -\omega_{sc}/13 & 0 & \omega_{sc}/11 \end{bmatrix} \vec{q} \quad (2a)$$

B. Nonlinear Attitude Dynamics Model
This study uses a nonlinear rigid-body attitude dynamics model in many of its simulations. It includes kinematic and dynamic equations of motion:

This study uses two orbital models. One is a Keplerian model that includes the secular perturbations caused by the Earth's $\frac{1}{2}$ oblate-ness term. Its mathematical form is presented in the appendix of Ref. 19. The second model is a simple circular model that neglects all oblateness effects. It is used for analysis and design calculations that need to execute rapidly.

A model of the spacecraft's orbit is used to compute four important quantities: the instantaneous Earth-relative position of the spacecraft $\mathbf{r}_{CEC}(t)$, the instantaneous Earth-relative velocity of the spacecraft $\mathbf{v}_{CEC}(t)$, the inertial rotation rate of the local-level reference frame $\mathbf{\omega}_{LL}(t)$, and the orientation parameters of the local-level coordinate system $\mathbf{A}_{LL}^{(1)}(t)$. These quantities depend on the Kepler parameters of the orbit, and they transform from local-level coordinates $\mathbf{A}_{LL}^{(1)}$ to ECEF coordinates $\mathbf{A}_{ECEF}^{(1)}$ through the transformation matrix \mathbf{M}_{LE} .

The other important reference frame is spacecraft body-fixed. When nadir-pointing spacecraft has the desired attitude, this body-fixed reference frame is aligned with the local-level reference frame. Deviations of this reference frame from the local-level reference frame are referred to as roll, pitch, and yaw. The attitude matrix from local-level to inertial coordinates is given by

In the case of a nadir-pointing spacecraft, it is traditional to define vehicle's orientation relative to the local-level coordinate system, which follows the spacecraft around its orbit. The local-level system's +z axis points toward nadir and its y axis is perpendicular to both the nadir vector and the instantaneous orbital velocity vector. The +x axis is defined by the right-hand rule, points approximately along the orbital velocity vector.

II. Models of the Magnetic Attitude Control Problem

attitude control problem, and it presents analysis and simulation results for the closed-loop system.

$$P_k = P_{k(0)} + e^k P_{k(1)} + e^{2k} P_{k(2)} + \dots \quad \text{for } k = 1, 2, 3, \dots \quad (12c)$$

$$P_k = P_{k(0)} + e^k P_{k(1)} + e^{2k} P_{k(2)} + \dots \quad \text{for } k = 1, 2, 3, \dots \quad (12b)$$

$$P_0 = e^{-1} P_{0(-1)} + P_{0(0)} + e^{0(1)} + e^{2} P_{0(2)} + \dots \quad (12a)$$

Next, express the Fourier coefficients of $P(t)$ as asymptotic series in the small quantity e :

This is possible because these two matrix time histories are periodic. The matrices P_0, P_k, B_0, B_k , and B_{sys} are constant Fourier coefficients.

Therefore, $P(t) = R_{-1}B_T(t)P_0 + \sum_{k=1}^{\infty} B_{sys}e^{2kt}$

$$+ B_{sys} \sin\left(\frac{2\pi kt}{T}\right) \quad (11b)$$

$$B(t)R_{-1}B_T(t) = B_0B_0 + \sum_{k=1}^{\infty} B_{sys} \cos\left(\frac{2\pi kt}{T}\right) \quad (11a)$$

as Fourier series:

representation of $P(t)$. Start by expressing $P(t)$ and $B(t)R_{-1}B_T(t)$ in terms of P_0 .

Proof. The proof uses a combined Fourier and asymptotic series which allows A to have complex conjugate pairs of eigenvalues.

Then $P(t) \rightarrow P_s$, a constant matrix, in the limit as the control eigenvalues.

Every eigenvalue of A is unique; that is, there are no repeated eigenvalues.

(4) A has no eigenvalues in the right-half plane.

(3) $[A, C]$ is observable, where $C = Q$ by definition.

(2) $[A, B_0]$ is stabilizable, where $B_0B_0 = (1/T) \int_0^T B(t)R_{-1}B_T(t) dt$ by definition.

(1) $R = R_0e^2$, where R_0 is positive definite.

Theorem. If the following conditions are met:

found by imposing the following periodic boundary conditions:

For an infinite-horizon problem the steady-state solution can be found by imposing the following time-varying boundary conditions:

The $P(t)$ matrix is the solution of the following time-varying Riccati equation:

To a Periodic Matrix Riccati Equation

B. Asymptotic Analysis of a Low-Bandwidth Solution

In summary, this paper varying component of its field vector, as in Ref. 7.

projection is accomplished by forming a cross product with the control input perpendicular to the local magnetic field. This

a scaled identity matrix, then multiplication by $R_{-1}B_T(t)$ projects under which such a P_s exists.

Riccati equation. The next subsection will demonstrate conditions P_s approximates the solution to a periodically time-varying matrix P , summands according to its formula in Eq. (6). The constant matrix

gain is the matrix $B(t), B(t)$ is constructed from magnetometer measurements

In summary, this paper varying component of its quasi-periodic $B(t)$ could be difficult.

periodic. Therefore, synchronization of a periodic $P(t)$ with the variations in $B(t)$. As already noted, the true $B(t)$ is not exactly

whole matrix. Furthermore, a constant P_s would not need to have its time variations synchronized with the actual time

if $P(t) = P_s$. A constant P_s would be much easier to store than a attractive force for use in a real system if $P(t)$ were even more

The control law $u(t) = -R_{-1}B_T(t)P(t)x(t)$ is only time-varying

in the Earth's magnetic field.

This allows the computed gain to compensate for uncertainty in the matrix. The model in Eq. (6) includes gravity-gradient effects, magnetohydrodynamic control forces, and disturbance forces, just as

as $R_{-1}B_T(t)P(t)$. In this case one can take advantage of the fact

that the gain matrix time history $K(t)$, it is better to express the gain magnetic-torque-based attitude control. Instead of computing a periodical law of this form is very useful in the context of stabilizing the system under appropriate conditions.²²

A control law for this form is given in the form of a time-

corresponding infinite horizon problem and leads to a periodic gain

the solution is equivalent to the steady-state solution of the chosen P_T the resulting $P(t)$ is periodic with period T . In this case

varying matrix Riccati equation.²² Furthermore, for a propagation

problem can be expressed in the form of a feedback control law:

i.e., $B(t) = B(t+T)$. It is well known that the solution to this state weighting matrix, and $B(t)$ is assumed to be exactly periodic,

where Q and R are constant weight matrices, P_T is the terminal

$$x(0) \text{ given} \quad (9d)$$

$$\dot{x} = Ax + B(t)u \quad (9c)$$

subject to:

$$J = \frac{1}{2} \int_0^T [x^T(t)Qx(t) + u^T(t)Ru(t)] dt + \frac{1}{2} x^T(T)P_T x(T) \quad (9b)$$

To minimize:

$$u(t) \quad \text{for } 0 \leq t \leq T \quad (9a)$$

Find:

Suppose one is given the periodic LQR problem.

A. Controller Design Requirements

Asymptotic Limit

III. Periodic LQR Design in the Low-Bandwidth

where t_m is the inclination of the spacecraft's orbit with respect to the magnetic equator and a is the orbit's semi-major axis. Time is measured from $t = 0$ at the ascending-node crossing of the magnetic field measured from $t = 0$ at the orbit's ascending node.

equator. The field's dipole strength is $u_f = 7.9 \times 10^{15} \text{ Wb-m}$.

the magnetic field from $t = 0$ at the orbit's semi-major axis. Time is measured from $t = 0$ at the orbit's ascending node crossing of the magnetic field measured from $t = 0$ at the orbit's ascending node.

A dipole approximation of the Earth's magnetic field, when cou-

pling as expressed in local-level coordinates:

The principal asymmetry is the center of the main dipole slightly away from the Earth's rotation axis.

The principal asymmetry is the cause of the main dipole slightly away from the Earth's rotation axis because of asymmetries in the Earth's magnetic field.

Earth rotation and orbit precession cause small deviations from this assumption and orbit rotation and no orbit pre-

cession, yields the following periodic model for the magnetic field with the assumptions of no Earth's magnetic field, when cou-

pling as expressed in local-level coordinates:

The time variations of this system can be approximated as being periodic: $b(t) = b(t+T)$ where $T = 2\pi/\omega_0$ is the orbital period.

The time variations of this system can be approximated as being periodic: $b_i(t) = b_i(t+T)$ where $T = 2\pi/\omega_i$ is the orbital period.

come from the time variations of the magnetic field components

control effectiveness matrix $B(t)$ is time varying. Its time variations

is the control vector, and $w = w_d$ is the disturbance vector. The ma-

trices $A, B(t)$, and B_w are effectively defined by Eq. (6). Only the

is the control vector, and $w = w_d$ is the state vector. The ma-

trices $A, B(t)$, and B_w are effectively defined by Eq. (6). Only the

is the control vector, and $w = w_d$ is the state vector. The ma-

trices $A, B(t)$, and B_w are effectively defined by Eq. (6). Only the

is the control vector, and $w = w_d$ is the state vector. The ma-

trices $A, B(t)$, and B_w are effectively defined by Eq. (6). Only the

is the control vector, and $w = w_d$ is the state vector. The ma-

trices $A, B(t)$, and B_w are effectively defined by Eq. (6). Only the

is the control vector, and $w = w_d$ is the state vector. The ma-

trices $A, B(t)$, and B_w are effectively defined by Eq. (6). Only the

is the control vector, and $w = w_d$ is the state vector. The ma-

trices $A, B(t)$, and B_w are effectively defined by Eq. (6). Only the

is the control vector, and $w = w_d$ is the state vector. The ma-

trices $A, B(t)$, and B_w are effectively defined by Eq. (6). Only the

is the control vector, and $w = w_d$ is the state vector. The ma-

trices $A, B(t)$, and B_w are effectively defined by Eq. (6). Only the

is the control vector, and $w = w_d$ is the state vector. The ma-

trices $A, B(t)$, and B_w are effectively defined by Eq. (6). Only the

is the control vector, and $w = w_d$ is the state vector. The ma-

trices $A, B(t)$, and B_w are effectively defined by Eq. (6). Only the

is the control vector, and $w = w_d$ is the state vector. The ma-

trices $A, B(t)$, and B_w are effectively defined by Eq. (6). Only the

is the control vector, and $w = w_d$ is the state vector. The ma-

trices $A, B(t)$, and B_w are effectively defined by Eq. (6). Only the

is the control vector, and $w = w_d$ is the state vector. The ma-

trices $A, B(t)$, and B_w are effectively defined by Eq. (6). Only the

is the control vector, and $w = w_d$ is the state vector. The ma-

trices $A, B(t)$, and B_w are effectively defined by Eq. (6). Only the

is the control vector, and $w = w_d$ is the state vector. The ma-

trices $A, B(t)$, and B_w are effectively defined by Eq. (6). Only the

is the control vector, and $w = w_d$ is the state vector. The ma-

trices $A, B(t)$, and B_w are effectively defined by Eq. (6). Only the

is the control vector, and $w = w_d$ is the state vector. The ma-

trices $A, B(t)$, and B_w are effectively defined by Eq. (6). Only the

is the control vector, and $w = w_d$ is the state vector. The ma-

trices $A, B(t)$, and B_w are effectively defined by Eq. (6). Only the

is the control vector, and $w = w_d$ is the state vector. The ma-

trices $A, B(t)$, and B_w are effectively defined by Eq. (6). Only the

is the control vector, and $w = w_d$ is the state vector. The ma-

trices $A, B(t)$, and B_w are effectively defined by Eq. (6). Only the

is the control vector, and $w = w_d$ is the state vector. The ma-

trices $A, B(t)$, and B_w are effectively defined by Eq. (6). Only the

is the control vector, and $w = w_d$ is the state vector. The ma-

trices $A, B(t)$, and B_w are effectively defined by Eq. (6). Only the

is the control vector, and $w = w_d$ is the state vector. The ma-

trices $A, B(t)$, and B_w are effectively defined by Eq. (6). Only the

is the control vector, and $w = w_d$ is the state vector. The ma-

trices $A, B(t)$, and B_w are effectively defined by Eq. (6). Only the

is the control vector, and $w = w_d$ is the state vector. The ma-

trices $A, B(t)$, and B_w are effectively defined by Eq. (6). Only the

is the control vector, and $w = w_d$ is the state vector. The ma-

trices $A, B(t)$, and B_w are effectively defined by Eq. (6). Only the

is the control vector, and $w = w_d$ is the state vector. The ma-

trices $A, B(t)$, and B_w are effectively defined by Eq. (6). Only the

is the control vector, and $w = w_d$ is the state vector. The ma-

trices $A, B(t)$, and B_w are effectively defined by Eq. (6). Only the

is the control vector, and $w = w_d$ is the state vector. The ma-

trices $A, B(t)$, and B_w are effectively defined by Eq. (6). Only the

is the control vector, and $w = w_d$ is the state vector. The ma-

trices $A, B(t)$, and B_w are effectively defined by Eq. (6). Only the

is the control vector, and $w = w_d$ is the state vector. The ma-

trices $A, B(t)$, and B_w are effectively defined by Eq. (6). Only the

is the control vector, and $w = w_d$ is the state vector. The ma-

trices $A, B(t)$, and B_w are effectively defined by Eq. (6). Only the

is the control vector, and $w = w_d$ is the state vector. The ma-

trices $A, B(t)$, and B_w are effectively defined by Eq. (6). Only the

is the control vector, and $w = w_d$ is the state vector. The ma-

trices $A, B(t)$, and B_w are effectively defined by Eq. (6). Only the

is the control vector, and $w = w_d$ is the state vector. The ma-

trices $A, B(t)$, and B_w are effectively defined by Eq. (6). Only the

is the control vector, and $w = w_d$ is the state vector. The ma-

trices $A, B(t)$, and B_w are effectively defined by Eq. (6). Only the

is the control vector, and $w = w_d$ is the state vector. The ma-

trices $A, B(t)$, and B_w are effectively defined by Eq. (6). Only the

is the control vector, and $w = w_d$ is the state vector. The ma-

trices $A, B(t)$, and B_w are effectively defined by Eq. (6). Only the

is the control vector, and $w = w_d$ is the state vector. The ma-

trices $A, B(t)$, and B_w are effectively defined by Eq. (6). Only the

is the control vector, and $w = w_d$ is the state vector. The ma-

trices $A, B(t)$, and B_w are effectively defined by Eq. (6). Only the

is the control vector, and $w = w_d$ is the state vector. The ma-

trices $A, B(t)$, and B_w are effectively defined by Eq. (6). Only the

is the control vector, and $w = w_d$ is the state vector. The ma-

trices $A, B(t)$, and B_w are effectively defined by Eq. (6). Only the

is the control vector, and $w = w_d$ is the state vector. The ma-

trices $A, B(t)$, and B_w are effectively defined by Eq. (6). Only the

is the control vector, and $w = w_d$ is the state vector. The ma-

trices $A, B(t)$, and B_w are effectively defined by Eq. (6). Only the

is the control vector, and $w = w_d$ is the state vector. The ma-

trices $A, B(t)$, and B_w are effectively defined by Eq. (6). Only the

is the control vector, and $w = w_d$ is the state vector. The ma-

trices $A, B(t)$, and B_w are effectively defined by Eq. (6). Only the

is the control vector, and $w = w_d$ is the state vector. The ma-

trices $A, B(t)$, and B_w are effectively defined by Eq. (6). Only the

is the control vector, and $w = w_d$ is the state vector. The ma-

trices $A, B(t)$, and B_w are effectively defined by Eq. (6). Only the

is the control vector, and $w = w_d$ is the state vector. The ma-

trices $A, B(t)$, and B_w are effectively defined by Eq. (6). Only the

is the control vector, and $w = w_d$ is the state vector. The ma-

trices $A, B(t)$, and B_w are effectively defined by Eq. (6). Only the

is the control vector, and $w = w_d$ is the state vector. The ma-

trices $A, B(t)$, and B_w are effectively defined by Eq. (6). Only the

is the control vector, and $w = w_d$ is the state vector. The ma-

trices $A, B(t)$, and B_w are effectively defined by Eq. (6). Only the

is the control vector, and $w = w_d$ is the state vector. The ma-

trices $A, B(t)$, and B_w are effectively defined by Eq. (6). Only the

is the control vector, and $w = w_d$ is the state vector. The ma-

trices $A, B(t)$, and B_w are effectively defined by Eq. (6). Only the

is the control vector, and $w = w_d$ is the state vector. The ma-

trices $A, B(t)$, and B_w are effectively defined by Eq. (6). Only the

the spacecraft inertial properties, and/or the magnetic field. Various types of parametric uncertainty between the model and the true system have been investigated. The orbital attitude has

C. Robustness with Respect to Parameteric System Uncertainty

An important aspect of any controller design is its tolerance of uncertainty in the open-loop system model that has been used to design it. This is especially so in the present situation. Simplifying assumptions have been made about the magnetic field model, yet underactuation causes the controller to rely on model predictions

C. Robustness with Respect to Parametric System Uncertainty

This response near the equilibrium is $a_0 = 8130$. The maximum magnitude for its one-orbit state transition matrix is 0.76. This system is not quite as fast as the other one. The maximum translates into a slowest time constant of 3.7 orbits and an upper bound on its 2% settling time of about 14 orbits. Similar to case A, the slowest mode is primarily roll-jaw motion. In contrast to case A, the chosen value of a_0 does not quite minimize the worst-case settling time—the minimizing a_0 would be about 16,000 in this case.

$$R = \text{diag}(4.9 \times 10^4, 4.9 \times 10^4, 4.9 \times 10^4) \quad (25b)$$

0.01, 0.01, 0.01, 1.0, 1.0, 1.0) (25a)

$$\mathcal{Q} = \text{diag}(1.5 \times 10^{-8}, 1.5 \times 10^{-8}, 1.5 \times 10^{-8},$$

The spacecraft for this second case has roll and pitch gravity-
gradient stability, but its yaw motion is neutrally stable. Its inertia
matrix is $I = \text{diag}(250, 250, 10) \text{ kg-m}^2$, and its rectangular form has
roll, pitch, and yaw dimensions of 0.5, 0.5, and 3.4 m, respectively.
It is in a circular orbit with an inclination of 57 degrees and an altitude
of 57 km. It is like the spacecraft that was considered in Ref. 7.
The weights that have been used to design this slow LQR controller

Configuration

The eigenvalues of the actual system state transition matrix are relatively near to those of the state transition matrix for the average-*i*-invariant closed-loop system whose LQR solution was used to determine P_{ss} . Recall that this time-invariant system is the one whose Riccati equation appears as Eq. (20). This nearness of the eigenvalues of the small amplitude motion, that minimizes the upper bound for small amplitude motion, is due to the fact that the absolute values of the eigenvalues of the closed-loop system's state transition matrix are on the order of one or two orbits.

startrated operation, i.e., when operating near the nadir-pointing equilibrium, fast controller response is achieved by scaling up the gain by the factor $\alpha = 2500$.

The units of Ω are $1/(\text{rad-s})^2$ for the first three diagonal elements, $1/\text{rad}^2$ for the middle three diagonal elements, and $(\text{rad})^2$ for the last three diagonal elements. The units of R are all $1/(a\text{mp-m}^2)$. During

$$R = \text{diag}(6.2 \times 10^7, 6.2 \times 10^7, 6.2 \times 10^7) \quad (24b)$$

0.1, 1.0, 0.1, 0.1, 1.0, 0.1) (24a)

The first spaccerraft for which a controller has been designed has three-aixs gravity-gradient stability. Its inertia matrix is $I = \begin{bmatrix} 8.7 & 0.6 & 0.5 \\ 0.6 & 0.7 & 0.7 \\ 0.5 & 0.7 & 0.7 \end{bmatrix}$ kg-m 2 . It is a box of dimensions 0.7 m along the roll axis, 0.6 m along the pitch axis, and 0.9 m along the yaw axis. Its orbit is circular with an altitude of 600 km and an inclination of 90 deg. An asymptotic periodic controller has been designed for this spaccerraft. It uses the design that accounts for control saturation. Its slow LQR controller, the one that gets used when far from the equilibrium, has been designed using the following cost weighting

B. Nominal Controller Designs for Two Different

The inclusion of integrators cannot eliminate the effects of time-varying disturbances. Such disturbances can arise from solar radiation pressure, from the effects of atmospheric drag torque of atmosphere density variations, and from any residual magnetic dipole moment.

$$x^{aue} = \begin{bmatrix} A \\ I_3 \times 3, 0 \\ 0 \end{bmatrix} + u \begin{bmatrix} B \\ 0 \\ 0 \end{bmatrix} + x^{aue} \begin{bmatrix} B(t) \\ 0 \\ 0 \end{bmatrix} \quad (23)$$

Then the augmented state-space model takes the form

$$x^i(t) \, dt \quad \text{for } i = 1, 2, 3$$

integrals of the attitude errors:

Integrators are often used in feedback control systems. They can eliminate the steady-state effects of constant disturbances. For the magnetic circuit problem the use of integrators is challenging because of the system's time variations and especially because of the underdetermination issue: One cannot totally control the effects of a constant three-axis disturbance torque because the magnetic torque is constant and the three-axis disturbance torque is periodic. This feature eliminates biases from the system.

IV. Application to the Magnetic Torgueer Attitude Control Problem

Even when the linear system model that is used to design $K(s)$ only an approximation of an original nonlinear system, it is reasonable to use the infinite gain margin of the time-varying LQR to develop this saturation logic. According to Eqs. (22a-22c), a large gain margin is required only in the region of state space that is near equilibrium of the nonlinear system. This is acceptable because the equilibrium model constitutes a good approximation of the nonlinear system in this region.

Finally if some of the repeated eigenvalues of A are on the imaginary modifiable theorem is true, then its proof is more complicated, especially if x has a component in the neutrally stable subspace of A , i.e., if

It is probably possible to relax assumption 5) of the theorem. If the reason for this is similar to the reasoning that has been applied to Eqs. (14), the fact that $\{P_{(0-1)}\}_{ij} = 0$ if either i or j is greater than p , when coupled with assumption 3) of the theorem, implies that Eqs. (11a) and (11b) and substitute the results into Eq. (10). Asymptotic decomposition, Substitute Eqs. (12a-12c) into Eq. (10), followed by a Fourier decomposition, we find that the solution of a Lyapunov equation for a stable (sub-) system.

This is the case because it is associated with the stable subspace P_{ss} , which is the effective definition of equivalence between $P(t)$ and P_{ss} , as already discussed. Note that forward to show that $\|P(t)x - P_{ss}x\| \leq O(\epsilon)$ for all $t \neq 0$, factor of ϵ is the j th power. Using this formula for $P(t)$ and the power of ϵ denotes an expression whose highest

$$P(t) = \begin{bmatrix} (1/\epsilon)P_{AA(-1)} + P_{AA(0)} & P_{AB(0)} + O(\epsilon) \\ P_{BA(0)} + O(\epsilon) & P_{BB(0)} + O(\epsilon) \end{bmatrix} \quad (18)$$

It is now possible to conclude the proof of the theorem. Suppose that $P_{AA(-1)}$ is the $p \times p$ upper left-hand block of $P_{(0-1)}$. Similarly, suppose that $P_{AA(0)}$ is the $p \times p$ upper right-hand block of $P_{(0)}$, and that $P_{AB(0)}$ is the $p \times n-p$ lower right-hand block of $P_{(0)}$. Then $P_{BB(0)}$ is the $(n-p) \times (n-p)$ lower left-hand block of $P_{(0)}$. Theorem 5) implies that max $|P_{AA(ij)}| < p$ for all i, j .

It is straightforward to show that this determinant is nonzero if

$$\left| \begin{array}{cc} \zeta_1 + \zeta_2 & -2\pi k/T \\ 2\pi k/T & \zeta_1 + \zeta_2 \end{array} \right| \neq 0 \quad (17)$$

This pair of equations has the unique solution $\{P_{ck(0)}\}_{ij} = 0$ and $\{P_{dk(0)}\}_{ij} = 0$ if and only if

$$-(2\pi k/T)\{P_{ck(0)}\}_{ij} = -\{P_{dk(0)}\}_{ij}(\zeta_i + \zeta_j) \quad (16a)$$

for all i and j such that $i > p$ or $j > p$ (16b)

$$(2\pi k/T)\{P_{ck(0)}\}_{ij} = -\{P_{dk(0)}\}_{ij}(\zeta_i + \zeta_j) \quad (16a)$$

for all i and j such that $i < p$ or $j < p$ (16b)

$$-(2\pi k/T)\{P_{ck(0)}\}_{ij} = -\{P_{dk(0)}\}_{ij}(\zeta_i + \zeta_j) \quad (16a)$$

for all i and j such that $i > p$ or $j > p$ (16b)

of A , it is positive definite because it is the solution of a Lyapunov equation for a stable (sub-) system.

Equations (13c) and (13d) can be used to show that $\{P_{ck(0)}\}_{ij} = 0$

and $\{P_{dk(0)}\}_{ij} = 0$ in this case. Eqs. (13c) and (13d) can be written in scalar component form as follows:

of A , it is positive definite because it is the solution of a Lyapunov

equation for a stable (sub-) system.

Fourier analysis dictates that, in each of the resulting equations, the right-hand side of the equation must be equal to the sum of the coefficients of $e^{2\pi ik/T}$ on the left-hand side. The same goes for the constant terms and for the sums of the coefficients of $\sin(2\pi kt/T)$.

If one recognizes that $R_{-1} = e^{2\pi ik/T}$, then this matching of powers of e and of cosine, sine, and constant terms yields the following relationships:

$\cos(2\pi kt/T)P_{ck(0)} = -P_{ck(0)}A - AP_{ck(0)} + P_{0(-1)}B_{dk(0)}P_{0(-1)}$ (13c)

$\cos(2\pi kt/T)P_{dk(0)} = -P_{dk(0)}A - AP_{dk(0)} + P_{0(-1)}B_{ck(0)}P_{0(-1)}$ (13d)

$0 = -P_{0(-1)}A - AP_{0(-1)} - Q + P_{0(-1)}B_{0}B_{T}P_{0(-1)}$ (13b)

$0 = -P_{0(-1)}A - AP_{0(-1)}$ (13a)

$0 = -P_{0(-1)}\cos(2\pi kt/T)$ terms:

$0 = -P_{0(-1)}\sin(2\pi kt/T)$ terms:

$0 = -P_{0(-1)}\cos(2\pi kt/T)$ terms:

$0 = -P_{0(-1)}\sin(2\pi kt/T)$ terms:

$0 = -P_{0(-1)}\cos(2\pi kt/T)$ terms:

$0 = -P_{0(-1)}\sin(2\pi kt/T)$ terms:

$0 = -P_{0(-1)}\cos(2\pi kt/T)$ terms:

$0 = -P_{0(-1)}\sin(2\pi kt/T)$ terms:

$0 = -P_{0(-1)}\cos(2\pi kt/T)$ terms:

$0 = -P_{0(-1)}\sin(2\pi kt/T)$ terms:

$0 = -P_{0(-1)}\cos(2\pi kt/T)$ terms:

$0 = -P_{0(-1)}\sin(2\pi kt/T)$ terms:

$0 = -P_{0(-1)}\cos(2\pi kt/T)$ terms:

$0 = -P_{0(-1)}\sin(2\pi kt/T)$ terms:

$0 = -P_{0(-1)}\cos(2\pi kt/T)$ terms:

$0 = -P_{0(-1)}\sin(2\pi kt/T)$ terms:

$0 = -P_{0(-1)}\cos(2\pi kt/T)$ terms:

$0 = -P_{0(-1)}\sin(2\pi kt/T)$ terms:

$0 = -P_{0(-1)}\cos(2\pi kt/T)$ terms:

$0 = -P_{0(-1)}\sin(2\pi kt/T)$ terms:

$0 = -P_{0(-1)}\cos(2\pi kt/T)$ terms:

$0 = -P_{0(-1)}\sin(2\pi kt/T)$ terms:

$0 = -P_{0(-1)}\cos(2\pi kt/T)$ terms:

$0 = -P_{0(-1)}\sin(2\pi kt/T)$ terms:

$0 = -P_{0(-1)}\cos(2\pi kt/T)$ terms:

$0 = -P_{0(-1)}\sin(2\pi kt/T)$ terms:

$0 = -P_{0(-1)}\cos(2\pi kt/T)$ terms:

$0 = -P_{0(-1)}\sin(2\pi kt/T)$ terms:

$0 = -P_{0(-1)}\cos(2\pi kt/T)$ terms:

$0 = -P_{0(-1)}\sin(2\pi kt/T)$ terms:

$0 = -P_{0(-1)}\cos(2\pi kt/T)$ terms:

$0 = -P_{0(-1)}\sin(2\pi kt/T)$ terms:

$0 = -P_{0(-1)}\cos(2\pi kt/T)$ terms:

$0 = -P_{0(-1)}\sin(2\pi kt/T)$ terms:

$0 = -P_{0(-1)}\cos(2\pi kt/T)$ terms:

$0 = -P_{0(-1)}\sin(2\pi kt/T)$ terms:

$0 = -P_{0(-1)}\cos(2\pi kt/T)$ terms:

$0 = -P_{0(-1)}\sin(2\pi kt/T)$ terms:

$0 = -P_{0(-1)}\cos(2\pi kt/T)$ terms:

$0 = -P_{0(-1)}\sin(2\pi kt/T)$ terms:

$0 = -P_{0(-1)}\cos(2\pi kt/T)$ terms:

$0 = -P_{0(-1)}\sin(2\pi kt/T)$ terms:

$0 = -P_{0(-1)}\cos(2\pi kt/T)$ terms:

$0 = -P_{0(-1)}\sin(2\pi kt/T)$ terms:

$0 = -P_{0(-1)}\cos(2\pi kt/T)$ terms:

$0 = -P_{0(-1)}\sin(2\pi kt/T)$ terms:

$0 = -P_{0(-1)}\cos(2\pi kt/T)$ terms:

$0 = -P_{0(-1)}\sin(2\pi kt/T)$ terms:

$0 = -P_{0(-1)}\cos(2\pi kt/T)$ terms:

$0 = -P_{0(-1)}\sin(2\pi kt/T)$ terms:

$0 = -P_{0(-1)}\cos(2\pi kt/T)$ terms:

$0 = -P_{0(-1)}\sin(2\pi kt/T)$ terms:

$0 = -P_{0(-1)}\cos(2\pi kt/T)$ terms:

$0 = -P_{0(-1)}\sin(2\pi kt/T)$ terms:

$0 = -P_{0(-1)}\cos(2\pi kt/T)$ terms:

$0 = -P_{0(-1)}\sin(2\pi kt/T)$ terms:

$0 = -P_{0(-1)}\cos(2\pi kt/T)$ terms:

$0 = -P_{0(-1)}\sin(2\pi kt/T)$ terms:

$0 = -P_{0(-1)}\cos(2\pi kt/T)$ terms:

$0 = -P_{0(-1)}\sin(2\pi kt/T)$ terms:

$0 = -P_{0(-1)}\cos(2\pi kt/T)$ terms:

$0 = -P_{0(-1)}\sin(2\pi kt/T)$ terms:

$0 = -P_{0(-1)}\cos(2\pi kt/T)$ terms:

$0 = -P_{0(-1)}\sin(2\pi kt/T)$ terms:

$0 = -P_{0(-1)}\cos(2\pi kt/T)$ terms:

$0 = -P_{0(-1)}\sin(2\pi kt/T)$ terms:

$0 = -P_{0(-1)}\cos(2\pi kt/T)$ terms:

$0 = -P_{0(-1)}\sin(2\pi kt/T)$ terms:

$0 = -P_{0(-1)}\cos(2\pi kt/T)$ terms:

$0 = -P_{0(-1)}\sin(2\pi kt/T)$ terms:

$0 = -P_{0(-1)}\cos(2\pi kt/T)$ terms:

$0 = -P_{0(-1)}\sin(2\pi kt/T)$ terms:

$0 = -P_{0(-1)}\cos(2\pi kt/T)$ terms:

$0 = -P_{0(-1)}\sin(2\pi kt/T)$ terms:

$0 = -P_{0(-1)}\cos(2\pi kt/T)$ terms:

$0 = -P_{0(-1)}\sin(2\pi kt/T)$ terms:

$0 = -P_{0(-1)}\cos(2\pi kt/T)$ terms:

$0 = -P_{0(-1)}\sin(2\pi kt/T)$ terms:

$0 = -P_{0(-1)}\cos(2\pi kt/T)$ terms:

$0 = -P_{0(-1)}\sin(2\pi kt/T)$ terms:

$0 = -P_{0(-1)}\cos(2\pi kt/T)$ terms:

$0 = -P_{0(-1)}\sin(2\pi kt/T)$ terms:

$0 = -P_{0(-1)}\cos(2\pi kt/T)$ terms:

$0 = -P_{0(-1)}\sin(2\pi kt/T)$ terms:

$0 = -P_{0(-1)}\cos(2\pi kt/T)$ terms:

$0 = -P_{0(-1)}\sin(2\pi kt/T)$ terms:

$0 = -P_{0(-1)}\cos(2\pi kt/T)$ terms:

$0 = -P_{0(-1)}\sin(2\pi kt/T)$ terms:

$0 = -P_{0(-1)}\cos(2\pi kt/T)$ terms:

$0 = -P_{0(-1)}\sin(2\pi kt/T)$ terms:

$0 = -P_{0(-1)}\cos(2\pi kt/T)$ terms:

$0 = -P_{0(-1)}\sin(2\pi kt/T)$ terms:

$0 = -P_{0(-1)}\cos(2\pi kt/T)$ terms:

$0 = -P_{0(-1)}\sin(2\pi kt/T)$ terms:

$0 = -P_{0(-1)}\cos(2\pi kt/T)$ terms:

$0 = -P_{0(-1)}\sin(2\pi kt/T)$ terms:

$0 = -P_{0(-1)}\cos(2\pi kt/T)$ terms:

$0 = -P_{0(-1)}\sin(2\pi kt/T)$ terms:

$0 = -P_{0(-1)}\cos(2\pi kt/T)$ terms:

$0 = -P_{0(-1)}\sin(2\pi kt/T)$ terms:

$0 = -P_{0(-1)}\cos(2\pi kt/T)$ terms:

$0 = -P_{0(-1)}\sin(2\pi kt/T)$ terms:

$0 = -P_{0(-1)}\cos(2\pi kt/T)$ terms:

$0 = -P_{0(-1)}\sin(2\pi kt/T)$ terms:

$0 = -P_{0(-1)}\cos(2\pi kt/T)$ terms:

$0 = -P_{0(-1)}\sin(2\pi kt/T)$ terms:

$0 = -P_{0(-1)}\cos(2\pi kt/T)$ terms:

$0 = -P_{0(-1)}\sin(2\pi kt/T)$ terms:

$0 = -P_{0(-1)}\cos(2\pi kt/T)$ terms:

$0 = -P_{0(-1)}\sin(2\pi kt/T)$ terms:

$0 = -P_{0(-1)}\cos(2\pi kt/T)$ terms:

$0 = -P_{0(-1)}\sin(2\pi kt/T)$ terms:

$0 = -P_{0(-1)}\cos(2\pi kt/T)$ terms:

$0 = -P_{0(-1)}\sin(2\pi kt/T)$ terms:

$0 = -P_{0(-1)}\cos(2\pi kt/T)$ terms:

$0 = -P_{0(-1)}\sin(2\pi kt/T)$ terms:

$0 = -P_{0(-1)}\cos(2\pi kt/T)$ terms:

$0 = -P_{0(-1)}\sin(2\pi kt/T)$ terms:

$0 = -P_{0(-1)}\cos(2\pi kt/T)$ terms:

$0 = -P_{0(-1)}\sin(2\pi kt/T)$ terms:

$0 = -P_{0(-1)}\cos(2\pi kt/T)$ terms:

$0 = -P_{0(-1)}\sin(2\pi kt/T)$ terms:

$0 = -P_{0(-1)}\cos(2\pi kt/T)$ terms:

$0 = -P_{0(-1)}\sin(2\pi kt/T)$ terms:

$0 = -P_{0(-1)}\cos(2\pi kt/T)$ terms:

$0 = -P_{0(-1)}\sin(2\pi kt/T)$ terms:

$0 = -P_{0(-1)}\cos(2\pi kt/T)$ terms:

$0 = -P_{0(-1)}\sin(2\pi kt/T)$ terms:

$0 = -P_{0(-1)}\cos(2\pi kt/T)$ terms:

$0 = -P_{0(-1)}\sin(2\pi kt/T)$ terms:

$0 = -P_{0(-1)}\cos(2\pi kt/T)$ terms:

$0 = -P_{0(-1)}\sin(2\pi kt/T)$ terms:

$0 = -P_{0(-1)}\cos(2\pi kt/T)$ terms:

$0 = -P_{0(-1)}\sin(2\pi kt/T)$ terms:

$0 = -P_{0(-1)}\cos(2\pi kt/T)$ terms:

$0 = -P_{0(-1)}\sin(2\pi kt/T)$ terms:

$0 = -P_{0(-1)}\cos(2\pi kt/T)$ terms:

$0 = -P_{0(-1)}\sin(2\pi kt/T)$ terms:

$0 = -P_{0(-1)}\cos(2\pi kt/T)$ terms:

$0 = -P_{0(-1)}\sin(2\pi kt/T)$ terms:

$0 = -P_{0(-1)}\cos(2\pi kt/T)$ terms:

$0 = -P_{0(-1)}\sin(2\pi kt/T)$ terms:

$0 = -P_{0(-1)}\cos(2\pi kt/T)$ terms:

$0 = -P_{0(-1)}\sin(2\pi kt/T)$ terms:

$0 = -P_{0(-1)}\cos(2\pi kt/T)$ terms:

$0 = -P_{0(-1)}\sin(2\pi kt/T)$ terms:

$0 = -P_{0(-1)}\cos(2\pi kt/T)$ terms:

$0 = -P_{0(-1)}\sin(2\pi kt/T)$ terms:

$0 = -P_{0(-1)}\cos(2\pi kt/T$

where $\alpha_0 \rightarrow 1$ is the scaling factor that increases the response speed near the equilibrium and β is an inverse scaling factor that is used to stabilize the sped-up system with its saturation region of state space that is shown to be the same large region of state space that is guaranteed to be stable for the slow controller is used.

$$n_{\text{nom}} = \begin{cases} (1/\beta)n_{\text{nom}} & \text{if } \beta \leq 1 \\ 1 < \beta & \text{if } \beta > 1 \end{cases} \quad (22c)$$

$$g = \max_i \frac{(u_{\max})_i}{(u_{\text{nom}})_i} \quad (22b)$$

$$u_{\text{nom}} = -\alpha_0 R_{-1} B_1(t) P^{ss} x \quad (22a)$$

The technique goes on to use the infinite gain margin of the LQR in order to recover good performance near the equilibrium. It does this by scaling the control law by a factor $\alpha > 1$. If first strictes a value of α that is much larger than 1, call this α_0 . If this produces a control input that does not violate any of the bounds $|u(t)| \leq u_{\max}$, then α_0 is used. Otherwise, it scales down α_0 until all of the feedback control inputs respect all of the saturation bounds.

This same technique can be used for the problem at hand. A time-varying LQR of the form $u = -K(x)u + B(x)w$ has the same gain margin as a time-invariant LQR. [It is easy to demonstrate this by using the Lyapunov function $V = 0.5x^T P x$ along with Eq. (10) to show that $\dot{V} \leq 0$ for all x in the range $0.5 < a < \infty$.] For any $a > 1$ a modified time-varying control law of the form $u = -K(x)u + B(x)w$ solution to a modified time-varying LQR problem and will stabilize the system. To design this control saturation logic, the asymptotic periodictic LQR starts by using a very large R matrix in its design. This yields a P_s matrix and a control law $u = -R^{-1}B^T(1/P_s)x$ that satisfies the no-control-saturation criterion in a very large region of state space. The speed the system response near the state-space origin, the control law scales up the gain according to the following rules:

Reference 24 designs an initial LQR that has a very low bandwidth. It the system has no open-loop eigenvalues in the right-half plane, then K can be made arbitrarily small by this method, and the nominal LQR control law can be made to function stably in arbitrary large region of state space without violating any of the bounds $\|u\|_1 \leq u_{\max}$. Unfortunately, the resulting controller will have poor performance close to the origin if one of the state space because

Reference 24 presents a method for dealing with control saturation in the context of time-invariant LQR controllers. Its approach exploits the fact that an LQR-based controller has infinite gain margin. That is, if the control law $u = -Kx$ stabilizes the system and it has been computed by solving an LQR problem, then the control u has been computed by solving an LQR problem.

Central saturation occurs when any component of the complete vector exceeds the maximum that is permitted by the attributes, i.e., $|u_i| > u_{max}^i$, for some i . Any practical controller must be designed to behave stably if this occurs. It is not always obvious how to deal with such a situation, especially if the feedback controllers include time delays.

3. Design for Control Saturation

Such systems can be expected to have a degree of robustness with respect to system modeling errors. This is true because the controllers are approximated by full-state feedback LQRs. Time-invariant LQRs are known to possess certain robustness properties.²¹ This robustness should carry over into the low bandwidth time-varying case because it is similar to a time-invariant system. In the case of the magnetic-torque-based attitude control system, where there is even more reason to expect robustness. This is so because the B_T^T matrix that is used in the control law is derived from magnetometer data, which contains very little modeling error, only that which results from small measurement inaccuracies.

A good way to design the controller is to pick the weighting matrices Q and R , compute P_{ss} , evaluate the closed-loop stability, and tune R accordingly. If the system is unstable, then R must be increased. The closed-loop system model is $\dot{x} = (A - B_1(R_1 - B_1^T P_{ss})x$. This is a periodic model, and its stability can be evaluated via Floquet analysis.²³ Floquet stability analysis consists of the closed-loop state transition matrix for one period of the system and verifies that all of its eigenvalues have a complex magnitude less than unity. One can use Floquet analysis to tune Q and R . One might optimize the speed of response by minimizing the maximum magnitude of the eigenvalues of the closed-loop state transition matrix.

It is a good idea to check the stability of the resulting closed-loop system. The theorem only says things about the limiting small behavior of the system. It says nothing about what constitutes a small loop performance. If it remains stable, then the system response is likely to be faster for a larger value of ϵ because this involves less control effort.

After-the-Fact Flouquet Analysis

This controller design technique is similar to one that is employed in Ref. [1]. There are two main differences. First, Ref. [1] squares the $B_i(t)$ control effectiveness matrix twice, once before averaging and once when it gets used in the time-invariant Riccati equation. Second, Ref. [1] makes no attempt to relate the solution of its time-invariant LQR problem to the asymptotic low-bandwidth solution of a periodically time-varying problem. This relationship can be an important aid to the development of a method for dealing with the case of state or density.

where T is the nominal orbital period. The square-root factorization of the integral can be computed using an eigenvaluate decomposition. The rank of (ϵB_0) can be greater than the instantaneous rank of $B(t)$. An asymptotic analysis of this P_{ss} shows that $\|(\epsilon^{-1}P_{ss})^{(0,-1)} + P_{ss}^{(0)}x - P_{ss}^{(0)}\|$ is on the order of $\epsilon \|(\epsilon^{-1}P_{ss}^{(0,-1)} + P_{ss}^{(0)})x\|$, which means that, for small ϵ , the new form of P_{ss} is equivalent to the form used in the proof. This analysis expands the new P_{ss} in an asymptotic series in ϵ . This is true in the magnetic torque control problem.

$$\{e^B B^0\} e^B = \frac{1}{I} \int_1^0 B(\tau) R_{-1} B_T(\tau) d\tau \quad (21)$$

This equation can be solved using standard software packages. The control effectiveness matrix is (E^0_0) , and the control cost weightings matrix is (e^0_0) . From assumptions 1) and 2) of the theorem, it is possible to calculate (e^0_0) from a square-root factorization of the average weighted square of $B(i)$:

$$0 = -P^{ss}A - A_1 P^{ss} - \bar{Q} + P^{ss}(eB^0)(eB^0)^\top P^{ss} \quad (20)$$

A slightly different approximation of the matrix P , can be determined by solving the following steady-state time-invariant Riccati equation:

The key idea of this theorem is that the closed-loop system responds relatively slowly compared to the system period T . In this case $P(t)$ does not vary rapidly over one period. Therefore, it cannot vary much from its average value, which is P_{av} .

expansion of P_0 is $\epsilon^{-1}(1/\epsilon)$, where ϵ is the maximum number of repetitions of an eigenvalue that is on the imaginary axis.

axis. In this case the lowest power of ϵ that appears in the asymptotic

C. Robustness with Respect to Parameter System Uncertainty

$$R = \text{diag}(4.9 \times 10^4, 4.9 \times 10^4, 4.9 \times 10^4)$$

$$0.001, 0.01, 0.01, 1.0, 1.0, 1.0, 1.0) \quad (25a)$$

$$Q = \text{diag}(1.5 \times 10^{-8}, 1.5 \times 10^{-8}, 1.5 \times 10^{-8}),$$

The spacecraft for this second case has roll and pitch gravity-
gradient stability, but its yaw motion is neutrally stable. Its inertia
matrix is $I = \text{diag}(250, 250, 10) \text{ kg-m}^2$, and its rectangular form has
dimensions of 0.5, 0.5, and 3.4 m, respectively.
The spacecraft has roll and pitch gravitational
weights that have been used to design its slow LQR controller
at 657 km. It is like the spacecraft that was considered in Ref. 7,
but it is in a circular orbit with an inclination of 57 deg and an altitude
of 657 km, and yaw dimensions of 0.5, 0.5, and 3.4 m, respectively.

The eigenvalues of the actual system state transition matrix are off-orbit state transition matrix. Relatively near to those of the state transition matrix for the averaged time-invariant solution whose LQR solution was used to determine P_{ss} . Recall that this time-invariant system is the one whose Riccati equation appears as Eq. (20). This normless of eigenvalues demonstrates that the time-varying model is reasonably good approximation of the time-varying system when closed-loop time constants are on the order of one or two orbits.

The fast response of this periodic system is good. Its one-orbit wave-controller's gain by the factor $a_0 = 250$.

The units of Q are $1/\text{rad} \cdot \text{s}^2$ for the first three diagonal elements, $1/\text{rad}^2$ for the middle three diagonal elements, and $\text{N} \cdot \text{rad}$ for the last three diagonal elements. The units of R are all $1/(amp \cdot m^2)$. During

$$R = \text{diag}(6.2 \times 10^7, 6.2 \times 10^7, 6.2 \times 10^7)$$

(z₁₋₄) 0.1, 1.0, 0.1, 0.1, 1.0, 0.1)

$$\bar{Q} = \text{diag}(1.5 \times 10^{-6}, 1.5 \times 10^{-6}, 1.5 \times 10^{-6})$$

The first spacecraft for which a controller has been designed has three axes gravity-gradient stability. Its inertia matrix is $I = \begin{bmatrix} 7 & 0 & 0 \\ 0 & 10 & 0 \\ 0 & 0 & 15 \end{bmatrix}$ kg-m 2 . It is a box of dimensions 0.7 m along the roll axis, 0.6 m along the pitch axis, and 0.9 m along the yaw axis. Its orbit is circular with an altitude of 600 km and an inclination of 90 deg. An asymmetric periodic controller has been designed for this spacecraft; it uses the design that accounts for control saturation. Its slow LQR controller, the one that gets used when far from the equilibrium, has been designed using the following cost weighting:

B. Nominal Controller Designs for Two Different Spacecraft Configurations

The inclusion of megafalloids cannot eliminate the effects of time-variations of disturbance. Such disturbances can arise from solar radiation pressure, from the effects on the drag torque of atmospheric variations, and from any residual magnetic dipole moment.

where the matrices A , $B^{(1)}$, and $B^{(2)}$ are the same as in Eqs. (6) and (7). This system is a periodic time-varying linear system of the same form as in Eq. (9c). Although assumption 5 of the theorem is violated by the repeated eigenvalues at the origin, comparison of the difference has shown that this system admits the design of asymptotic controllers.

$$x_{\text{aug}} = \begin{bmatrix} 0 \\ 0 \end{bmatrix} + \begin{bmatrix} B^{(0)} \\ 0 \end{bmatrix} + \begin{bmatrix} B^{(1)} \\ 0 \end{bmatrix} + \dots + \begin{bmatrix} A \\ 0 \end{bmatrix} = \begin{bmatrix} 0 \\ [I_3 \times 3, 0] \end{bmatrix} x_{\text{aug}} \quad (23)$$

Then the augmented state-space model takes the form

$$x^i(t) \, dt \quad \text{for } i = 1, 2, 3$$

integrals of the attitude errors:

Integrators are often used in feedback control systems. They can eliminate the steady-state effects of constant disturbances. For the analogous attitude control problem the use of integrators is challenging because of the system's time variations and especially because of the underactuation issue: One cannot totally counteract the effects of constant three-axis disturbances torque because the magnitude of each effect is proportional to the control effort. This feature eliminates pointings biases from the system.

The asymmetric periodic LQR technique has been applied to the magnetic-torquer-based attitude control design problem. This section describes how it has been applied, and it presents analysis and simulation results for two different spacecraft configurations.

IV. Application to the Magnetic Torquer

Even when the linear system model that is used to design K (1) is only an approximation of an original nonlinear system, it is reasonable to use the infinite gain margin of the time-varying LQR to develop this saturation logic. According to Eqs. (22a–22c), a large gain margin is required only in the region of state space that is near the equilibrium of the nonlinear system. This is acceptable because the linearized model constitutes a good approximation of the non-linear system in this region.

The response of system B to large initial errors is depicted in Fig. 3. As in Fig. 1, the initial attitude errors are about 30 deg on all three axes, and the initial rate errors are about 30 deg/sec. The response of system B to large initial errors is depicted in Fig. 3. As in Fig. 1, the initial attitude errors are about 30 deg on all three axes, and the initial rate errors are about 30 deg/sec. The response of system B to large initial errors is depicted in Fig. 3. As in Fig. 1, the initial attitude errors are about 30 deg on all three axes, and the initial rate errors are about 30 deg/sec. The response of system B to large initial errors is depicted in Fig. 3. As in Fig. 1, the initial attitude errors are about 30 deg on all three axes, and the initial rate errors are about 30 deg/sec.

The simulation demonstrates the controller's robustness. The residual system's oscillations after 0.5 h are caused by the disturbance torque. The average drate torque is 1.6×10^{-7} N-m about the yaw axis, which is about the pitch axis and 1.0×10^{-7} N-m about the yaw axis, which is somewhat constant for this configuration. In addition, there are oscillatory disturbances from the drags (caused by the orbital eccentricity of 0.002) and from a residual magnetic dipole moment. These oscillatory torques have peak-to-peak amplitudes as large as 3×10^{-7} N-m. The closed-loop steady-state response is unbiased on all three axes with maximum pitch and roll errors of 0.7 deg and a maximum yaw error of 1 deg. In open-loop operation the mean drag torque alone would have produced mean roll, pitch, and yaw errors of 0.5, and 7.8 deg, respectively. This controller greatly improves the system's yaw accuracy at the expense of slightly increased roll.

Fig. 2 presents the corresponding magnetic dipole moment feed-back control input time histories. This case is one that starts with a large initial attitude error, about 30 deg per axis, and with initial attitude rate errors in the range -0.03 to +0.03 deg/s. These rate errors are on the order of half the orbital rate. These rate errors cause controller saturation, as evidenced on Fig. 2—the conditions cause control saturation in this case. Nevertheless, the system converges to its equilibrium response in a little more than 0.03 amp-m^2 .

Fig. 2 Control input time histories for the system A example that starts with 30-degree initial pointing errors on all three axes.

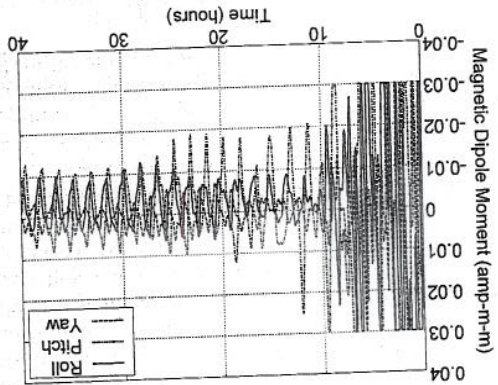
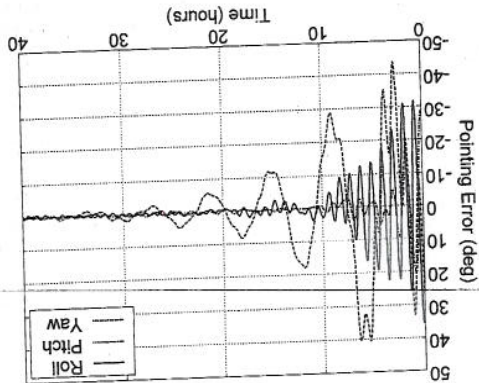


Fig. 1 System A pointing error time histories that start with 30-degree initial errors on all three axes.



A number of nonlinear simulations have been run for cases A and B. The nonlinear simulations test four aspects of system behavior: 1) its response to the real magnetic field of the rotating Earth; 2) the effects of which is not a dipole and which is not quite periodic; 2) the effects of nonlinearities of Eqs. (2a) and (2b) and the control saturation non-linearity of Eqs. (22a-22c); 3) its ability to counteract disturbance torques such as those caused by drag and by residual magnetic dipole moments; and 4) the impact of small orbital perturbations such as eccentricity and the eccentricity effect.

Both systems perform well in a wide range of situations. They both show good transient responses that agree with the predictions of their linear models when not in a saturated situation. Both systems are able to converge from large initial attitude and rate errors. These large initial conditions test both the functioning of the control saturation logic and the efficacy of linear control of this nonlinear system. Both controllers showed good steady-state response to disturbance torque inputs.

A simulation example of the case A system is presented in Figs. 1 and 2. Figure 1 presents the role, pitch, and yaw angle time histories, and Fig. 2, the nonlinear simulations test for the case of the rotating Earth. A simulation example of the case A system is presented in Figs. 1 and 2. Figure 1 presents the role, pitch, and yaw angle time histories, and Fig. 2, the nonlinear simulations test for the case of the rotating Earth.

Nonlinear Simulation Results

The bottom line on robustness is that the system has been shown to remain stable for a wide range of initial and internal variations if one nominally closed-loop response has been designed to be relatively insensitive. When very large state perturbations cause extreme levels of control saturation to occur, then in some cases the resultant slow system will be somewhat less robust to parameter uncertainty. At these large state perturbations the system is likely to experience other problems as well, problems such as large modeling errors as a result of a breakdown of the linearization assumption that has been used to derive the control law.

Both cases exhibit robust stability for all of the parameter sets that have been considered, 16 sets per case. In all mismodeling situations the fast-system closed-loop state transition matrix is stable—call that the fast system is the one that uses α to speed up the response. The slow system, the effective system when large amplitude response, causes extreme control saturation, is stable for most of the parameter sets that have been tried. For the case A system the slow system is stable for all parameter variations. The case B system exhibits instability in three scenarios, but instability occurs only for very large state amplitudes that cause the inverse scaling factor β to be 127 or greater—recall Eqs. (22a–22c). One scenario is when the true altitude is 100 km higher than the modeled altitude, and the other two scenarios occur when the yaw inertia factor is when the yaw varies by ± 0.1 away from its modeled value.

This study has considered two types of discrepancy between the detailed and truth magnetic fields. One is a perturbation in its period length to destabilize the open-loop system:

In perturbed ± 100 km, The orbital inclination has been perturbed 0 deg for the case A system and ∓ 20 deg for the case B system— later system should not be expected to work for inclination perturbations that make its inclination too low because the system overall uncontrollable in pitch at zero inclination. Perturbations in merit levels of $\pm 30\%$ have been tried. Also tested have been perturbations in the ratios of principal inertias that range up to 5%. Some case A merit perturbations caused vibration period ratios that were as large as 43% of the corresponding nominal period. Some of the case B merit perturbations were large

References

Pisatik, M., L. Theiler, J. Bloch, J., Ryan, S., Dill, R., W., and Warren, A., "AELXIS Spacecraft Attitude Reconstruction with Thermal/Flexible Modes Due to Launch Damage," *Journal of Guidance, Control, and Dynamics*, Vol. 20, No. 5, 1997, pp. 1033-1041.

Fox, S., M., Pisatik, P. K., Pisatik, M. L., and Moak, M. E., "Magnetic Attitude Determination Subsystems Performance of the LAGE Spacecraft," *Guidance and Control Conf. Conference*, Vol. 7A, edited by R. D. Cliff and J. P. McQuerry, University, San Diego, CA, 1991, pp. 553-574.

Yoshida, H., and Niimiyama, K., "A New Approach to Magnetic Attitude Measurement for Large Scientific Satellites," *NEC Research and Development*, Vol. 37, No. 1, 1996, pp. 60-77.

Ferranti, L., D. D., and da Cunha, J. J., "Attitude and Spin Rate Control of a Spinning Satellite Using Geomagnetic Field," *Journal of Guidance, Control and Dynamics*, Vol. 14, No. 1, 1991, pp. 216-218.

Spirkeau, M. E., "Optimal Periodic Control for Spacecraft Pointing and Attitude Determination," *Journal of Guidance, Control, and Dynamics*, Vol. 16, No. 6, 1993, pp. 1078-1084.

Martelli, F., Pisatik, P. K., and Pisatik, M. L., "Active Magnetic Control System Using Magnetic Sensors," *AIAA Journal*, Vol. 13, No. 6, 1975, pp. 817-822.

1988. Musser, K., L., and Ebter, W. L., "Autonomous Spacecraft Attitude Control Using Magnetic Torquing Only," *Proceedings of the Flight Mechanics Conference*, Vol. 17, No. 4, 1994, pp. 795-804.

1989. Seydel, W. H., "Comparison of Low-Earth-Orbit Satellite Attitude Controllers Submitted to Controllability Constraints," *Journal of Guidance, Control, and Dynamics*, Vol. 12, No. 1, 1989, pp. 23-38.

1990. Ardini, C., and Balloco, P., "Active Magnetic Attitude Control for Gravity Gradient Stabilized Spacecraft," *Journal of Guidance, Control, and Dynamics*, Vol. 13, No. 1, 1990, pp. 117-122.

References

Acknowledgment
This work was supported in part by the U.S. Air Force Office of Scientific Research Grant F49620-99-1-0169. Marc Jacobs was the lead investigator.

Acknowledgment

This technique has been applied to two example systems, both of which have only magnetic actuators and no wheels or gravity gradient booms. The controller's performance has been studied via analysis and simulation. The system has been shown to be robust in such systems by increasing the pointing accuracy of the momentum bias systems and other similar systems. They may prove useful like a thruster system.

The techniques developed in this paper also can be applied to momentum bias systems developed in this paper to a given level of accuracy.

This paper has shown how to design a class of stabilizing controllers for multi-pointing spacecraft. These controllers use only magnetic actuators. Their control laws are designed using a new type of periodic quadratic regulator whose Riccati equation solution is approximated by a linear time-invariant solution for an averaged system. The resulting full-state feedback controller derives its periodicity from the time-varying control influence matrix, which can be derived from the disturbance torques, and they employ a type of saturation logic - steady-state controllers use integrators in order to counteract 'steady-state disturbances' and they aim to gain margin property that maintains stability by using the infinite gain margin property that

V. Conclusions

will out this disturbance effect. Such an addition to the controller might be very important because residual dipole moments can be much larger than the levels used in this study.

In principle, a magnetic-torque-based controller should be able to dampen this type of oscillatory disturbance sort of estimator of the residual dipole moment in order to better completeley counteract this disturbance. It would need to use some as large as 10^{-10} A m .

oscillations will increase in amplitude as ϵ increases, but there will always be some minimum level of oscillation.

Much of the wave made its initial steady-state response in Fig. 4 results from the way in which this quasi-three-axis system deals with a true three-axis disturbance. In the process of nulling out the average effect of the constant drag torque, the controller induces oscillations. A good controller design will induce relatively small "side-effect" because the yaw mode is neutrally stable.

System B's steady-state response to disturbances is shown in Figure 4. This example has mean drag torques of 7.3×10^{-7} N-m about the pitch axis and 2.6×10^{-7} N-m about the yaw axis. The yaw mode is much lower. It would be infinity in open-loop operation but the error is caused by the drag torque in an open-loop situation, but the yaw mode is much lower. These roll and pitch errors are significantly larger than steady-state roll, pitch, and yaw errors at 0.6, 0.4, and 0.4 deg, respectively. These errors are significantly larger than steady-state roll, pitch, and yaw errors at 0.6, 0.4, and 0.4 deg, respectively. These roll and pitch errors are steady-state roll, pitch, and yaw errors at 0.6, 0.4, and 0.4 deg, respectively. These roll and pitch errors are steady-state roll, pitch, and yaw errors at 0.6, 0.4, and 0.4 deg, respectively. These roll and pitch errors are steady-state roll, pitch, and yaw errors at 0.6, 0.4, and 0.4 deg, respectively.

the controller converges to all in this case. Recall that the yaw mode for this design is neutrally stable. When combined with the internal action in the controller, the entire yaw subsystem is a series of three integrators. Such systems are very hard to stabilize when there is control saturation, even in the time-invariant case. What is more, the yaw mode's three repeated roots at the origin violate assumption 5) of the theorem. The ability to converge for this situation demonstrates that the proposed method is a powerful tool for wide controller design.

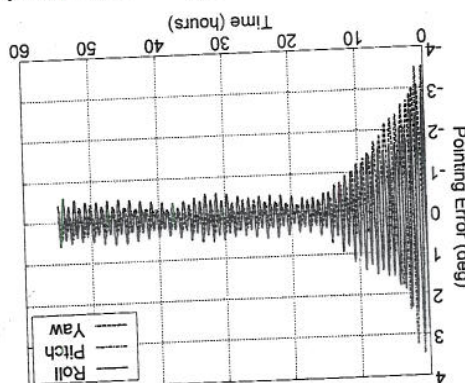
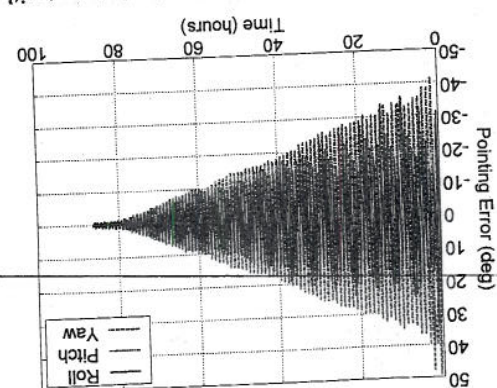


Fig. 3 System B pointing error time histories that start with 30-deg initial errors on all three axes.



The figure is a 3D surface plot titled "Pointing Error (deg)" on the vertical axis. The horizontal axis is labeled "Time (hours)" and ranges from 0 to 100. The depth axis represents the attitude axes: Roll, Pitch, and Yaw. The vertical axis ranges from -50 to 50 degrees. The surface shows a general upward trend in error over time, with more pronounced fluctuations in the Yaw axis.

00-0150 new

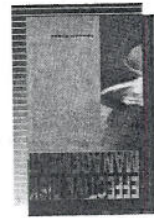
A and VA residents and applicable sales tax. For shipping and handling add \$15.00 per book or \$15.00 per order for higher quantities. All individual books—including U.S. postage—may be packed by themselves or combined in one order. Books may be shipped by UPS, FedEx, or USPS MailerCard or commercial freight companies. All individual books may be ordered at retail price and shipped to customers of commercial freight companies direct. International shipping and handling add \$15.00 per book or \$15.00 per order. Books may be shipped by UPS, FedEx, or USPS MailerCard or commercial freight companies. All individual books may be ordered at retail price and shipped to customers of commercial freight companies direct. International shipping and handling add \$15.00 per book or \$15.00 per order. Books may be shipped by UPS, FedEx, or USPS MailerCard or commercial freight companies.

2000 338 pp. Hardcover • ISBN 1-56347-383-6 • List Price: \$79.95 • AIAA Member Price: \$59.95 • Source Code: 945

- **Content:** Practice - Introduction and Need for Risk Management • Risk Management Overview • Risk Planning and Implementation • Risk Identification • Risk Monitoring and Control • Risk Mitigation • Risk Handling • Risk Mitigation • Risk Program • Risk Management and Milestones • Comparison of the Microeconomic Framework to Actual DOD Programs • Characteristics of the Cost-Performance Models of the Technique Possibility Surface • Program Structure Models • Sample Language for Including Risk Management in an RFP and Evaluating it During Selection • Characteristics and Limitations of Ordinary Scales in Risk Analysis • Example Technical Risk Analysis • Estimate Probabilities for Subjective Probability Statements.

This important new text defines the steps to effective risk management and helps the readers create a viable risk management process and implement some of their specific procedures. It will also allow the reader to better evaluate an existing risk management process, find some of the shortfalls, and develop and implement needed enhancements.





Edmund H. Corrigan

Effective Risk Management: Some Keys to Success

—Harold Kelenzner, Ph.D., Professor of Systems Management, Baldwin-Wallace College

"...easy to read, practical, and comprehensive. All facets of risk management are covered.... This book is a must..."

- 11 Wisniewski, R., "Linear Time Varying Approach to Satellite Attitude Control Using Only Electromagnetic Actuation," Proceedings of the AIAA Guidance, Navigation, and Control Conference, Vol. 23, AIAA, Reston, VA, 1997, pp. 24-31.

12 Wang, D., and Shekelle, Y. B., "Satellite Attitude Control Using Only Magnetic Torqueless," Proceedings of the AIAA Guidance, Navigation, and Control Conference, Vol. 23, AIAA, Reston, VA, 1997, pp. 1490-1498.

13 Curti, F., and Dianin, F., "Study on Active Magnetohydrodynamic Control for Lattice Spacecraft Bus MTTA," Proceedings of the 14th International Conference on Space Flight Dynamics, Special Issue of the Journal of the Brazilian Society of Mechanical Sciences, Vol. 21, 1999, pp. 432-444.

14 Wisniewski, R., and Blanke, M., "Fully Magnetic Attitude Control for Satellite Standard Atmosphere, 1976, National Oceanic and Atmospheric Administration, Washington, DC, 1976, pp. 50-73.

15 Kristiansen, H., McCalmaroch, N. H., and Rehyahoglu, M., "Attitude Stabilization of a Rigid Spacecraft Using Two Momentum Wheel Actuators," Journal of Guidance, Control, and Dynamics, Vol. 18, No. 2, 1995, pp. 256-263.

16 Tsiotras, P., Cofresi, M., and Longuski, J. M., "A Novel Approach to the Attitude Control of Asymmetric Spacecraft," Automatica, Vol. 31, No. 8, 1995, pp. 1099-1112.

17 Motrin, P., and Samson, C., "Time-Varying Exponential Stabilization of a Rigid Spacecraft with Two Control Torques," IEEE Transactions on Automatic Control, Vol. 42, No. 4, 1997, pp. 528-534.

18 Weritz, J. R. (ed.), "Spacecraft Attitude Determination and Control," D. Reidel, Boston, 1978, pp. 414, 779-786.

19 Pisaki, M. I., "Autonomous Orbit and Magnetic Field Determination Using Magneticometer and Star Sensors Data," Journal of Guidance, Control, and Dynamics, Vol. 18, No. 3, 1995, pp. 584-592.

20 United States Committee on Extension to the Standard Atmosphere, U.S. Standard Atmosphere, 1976, National Oceanic and Atmospheric Administration, Washington, DC, 1976, pp. 50-73.

21 Sengel, R. F., Optimal Control and Estimation, Dover, New York, 1994, pp. 270-272, 571-602.

22 Pastor, A., and Hemerle, V., "Differential Periodic Riccati Equations: Existence and Uniqueness of Nonnegative Definite Solutions," Mathematics of Control Signals and Systems, Vol. 6, No. 4, 1993, pp. 341-362.

23 Karlaftis, T., Linear Systems, Prentice-Hall, Upper Saddle River, NJ, 1980, p. 608.

24 Saberi, A., Lin, Z., and Teel, A. R., "Control of Linear Systems with Standard Actuators," IEEE Transactions on Automatic Control, Vol. 41, No. 3, 1996, pp. 368-378.